Shaped charge jet penetration reduction with increasing stand-off

GUNNAR WIJK, ANDERS TJERNBERG

FOI is an assignment-based authority under the Ministry of Defence. The core activities are research, method and technology development, as well as studies for the use of defence and security. The organization employs around 1350 people of whom around 950 are researchers. This makes FOI the largest research institute in Sweden. FOI provides its customers with leading expertise in a large number of fields such as security-policy studies and analyses in defence and security, assessment of different types of threats, systems for control and management of crises, protection against and management of hazardous substances, IT-security an the potential of new sensors.

FOI
Defence Research Agency
Weapons and Protection
SE-147 25 Tumba

Phone: +46 8 555 030 00
Fax: +46 8 555 031 00

www.foi.se

FOI-R-- 1750 --SE
ISSN 1650-1942

Weapons and Protection
Scientific report

November 2005

Shaped charge jet penetration reduction with increasing stand-off

FOI-R--1750--SE
ISSN 1650-1942

Weapons and Protection
Scientific report

November 2005

Issuing organization	Report number, ISRN	Report type
FOI – Swedish Defence Research Agency Weapons and Protection SE-147 25 Tumba	FOI-R--1750--SE	Scientific report
	Research area code 5. Strike and protection	
	Month year November 2005	**Project no.** E2007
	Sub area code 51 Weapons and Protection	
	Sub area code 2	

Author/s (editor/s)	Project manager
Gunnar Wijk Anders Tjernberg	Gunnar Wijk
	Approved by
	Sponsoring agency Swedish armed forces
	Scientifically and technically responsible

Report title

Shaped charge jet penetration reduction with increasing stand-off

Abstract

Penetration obtained with shaped charge (SC) jets decreases with increasing stand-off beyond optimum stand-off. The common explanation, namely that there is rotation and lateral dispersion of the fragments in the jets, cannot be the reason, at least not for precision shaped charges judging from flash photographs of such jets at stand-off distances that are several times the optimum stand-off. Instead it is suggested that the main reason is that previously eroded jet material in the hole erodes the remaining SC jet fragments on their way to the bottom of the hole. Computer simulation, in which eroded jet and target material are not immediately eliminated once they are eroded, shows that this explanation is qualitatively reasonable. Unfortunately it seems very difficult to design a quantitatively realistic physical model that accounts for this secondary erosion effect due the complicated nature of the interactions in question.

Keywords

Shaped charge jet, penetration, stand-off

Further bibliographic information	Language English
ISSN 1650-1942	**Pages** 15 p.
	Price acc. to pricelist

Utgivare FOI - Totalförsvarets forskningsinstitut Vapen och skydd 147 25 Tumba	**Rapportnummer, ISRN** FOI-R--1750--SE	**Klassificering** Vetenskaplig rapport
	Forskningsområde 5. Bekämpning och skydd	
	Månad, år November 2005	**Projektnummer** E2007
	Delområde 51 VVS med styrda vapen	
	Delområde 2	

Författare/redaktör Gunnar Wijk Anders Tjernberg	**Projektledare** Gunnar Wijk
	Godkänd av
	Uppdragsgivare/kundbeteckning Försvarsmakten
	Tekniskt och/eller vetenskapligt ansvarig

Rapportens titel

Modell för minskat inträngningsdjup med RSV med ökande detonationsavstånd till målet

Sammanfattning

Inträngningsdjupet för en RSV-stråle avtar med ökande detonationsavstånd (stand-off) när detta är större än det optimala detonationsavståndet. Den gängse förklaringen, nämligen att strålfragmenten börjar rotera och divergera i sidled, kan inte vara riktig, åtminstone inte för precisions-RSV om man skall döma av röntgenblixtfotografier av sådana strålar på avstånd som är flera gånger större än det optimala detonationsavståndet. I stället föreslås orsaken till avtagandet är att tidigare eroderade strålfragment i hålet eroderar de återstående fragmenten under de senares väg mot hålbotten. Numerisk simulering, varvid eroderat strål- och målmaterial inte omedelbart elimineras efter att ha eroderats, visar att denna förklaring är kvalitativt rimliig. Tyvärr förefaller det svårt att föreslå en kvantitativt realistisk modell som beaktar denna sekundära erosionseffekt.

Nyckelord

RSV, inträngning, stand-off

Övriga bibliografiska uppgifter	**Språk** Engelska
ISSN 1650-1942	**Antal sidor:** 15 s.
Distribution enligt missiv	**Pris: Enligt prislista**

Nomenclature

C	Shaped Charge (SC) calibre, m
D	SC insert diameter, m
D_T	hole diameter in target, m
$D_{T,\lim}$	limit hole diameter in target for *undisturbed* SC fragment erosion, m
d_P	diameter of SC jet fragment, m
h	SC insert thickness, m
L_P	accumulated length of SC jet, m
L	remaining length of SC jet, m
l_P	length of SC jet fragment, m
P	penetration depth, m
N	number of fragments
n	fragment number
S	stand-off distance, m
s	distance between fragments in a SC jet, m
u	penetration velocity, m/s
$u_{\lim}$	limit penetration velocity for *undisturbed* SC fragment erosion, m/s
V	SC insert volume, m^3
v	velocity of SC jet fragment, m/s
v_T	characteristic target velocity, m/s
$v_{\lim}$	limit fragment velocity for *undisturbed* SC fragment erosion, m/s
v_{front}	velocity of first SC jet fragment, m/s
Y_P	(uniaxial) yield strength of SC jet material, Pa
Y_T	(uniaxial) yield strength of target material, Pa
α	fraction of SC insert that becomes SC jet
β_P	jet fragment deformation coefficient
β_T	target penetration resistance coefficient
Λ_T	diameter of plastic deformation around an expanded hole, m
Ω	external target diameter, m
ψ_T	characteristic target velocity coefficient
ρ_P	density of SC jet material, kg/m^3
ρ_T	density of target material, kg/m^3
θ	SC insert half apex angle

Introduction

The relation in Figure 1 between shaped charge (SC) jet penetration depth and stand-off distance to the target is well known [1]. Initially, the penetration depth P increases with the stand-off distance S to a maximum value P_{opt} for an optimum stand-off distance S_{opt}. These quantities are normally proportional to the calibre C of the SC. Typical numerical values for a precision shaped charge (PSC) with a conical insert is $P_{opt} \approx S_{opt} \approx 6C$. More advanced SCs have "trumpet-like" inserts instead of cones and yield significantly larger maximum penetration without much change in the optimum stand-off distance. For a non-precision shaped charge (NPSC) the relations $P_{opt} \approx 2S_{opt} \approx 4C$ are representative. For $S > S_{opt}$ the penetration depth decreases with increasing stand-off S. The ideal jet performance of SCs in Figure 1 is never observed.

In the present paper only PSCs are considered. Radiographs of PSC jets show that they start to become fragmented at distances from the charge that are about equal to the optimum stand-off. For larger distances up to the maximum value in Figure 1, namely $S \approx 26C$, radiographs such as that shown in Figure 2 show that all fragments move along the same straight line and without any tendency for rotation when the jet is in free air. It is commonly assumed, for instance in [2], that lateral dispersion and fragment rotation are the main reasons for the decrease in penetration depth with increasing stand-off for $S > S_{opt}$. If this would be the explanation, however, then radiographs of undisturbed PSC jets should clearly reveal such behaviour. Accordingly some other explanation must be sought.

A fragmented SC jet is in principle a stream of small projectiles. The foremost fragment moves with the velocity v_{front} and the accumulated length of the fragments is L_P. The fragment velocity decreases along the

jet so that the velocity of a fragment, behind which the remaining accumulated length is L, is given by $v \approx v_{front} L/L_P$. A relevant model for projectile penetration should be able to describe SC jet penetration.

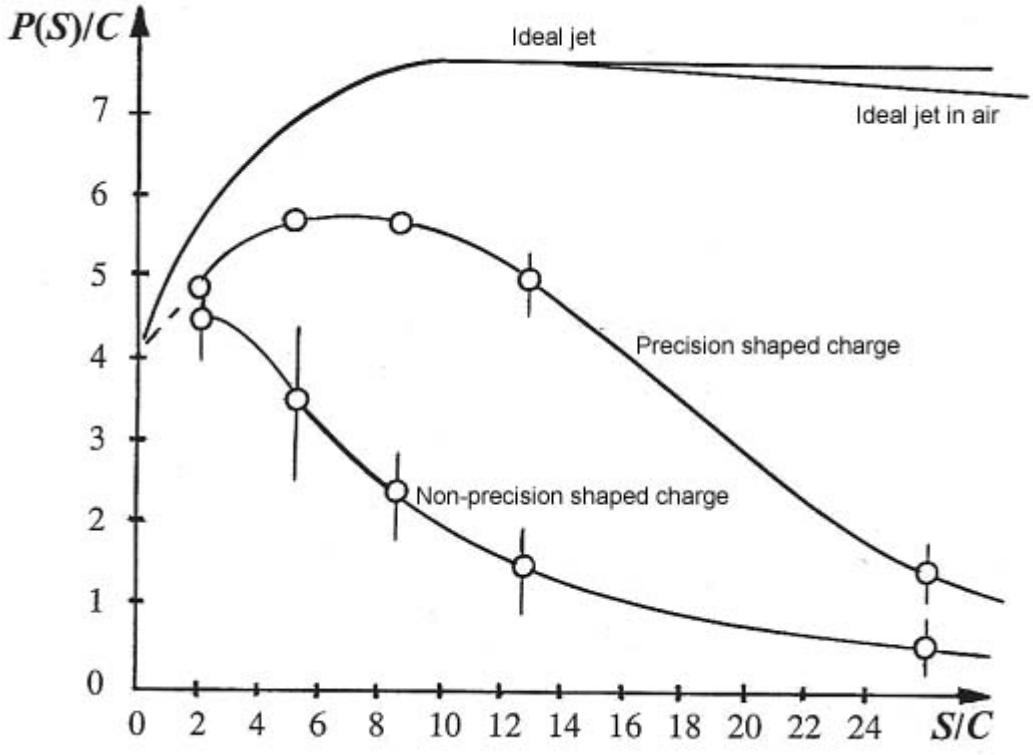

Figure 1: Stand-off curves for jets from SCs, of calibre *C* and with conical inserts, showing penetration *P* in steel armour as functions of stand-off distance *S* [mainly copied from 1: chapter 10, figure 4].

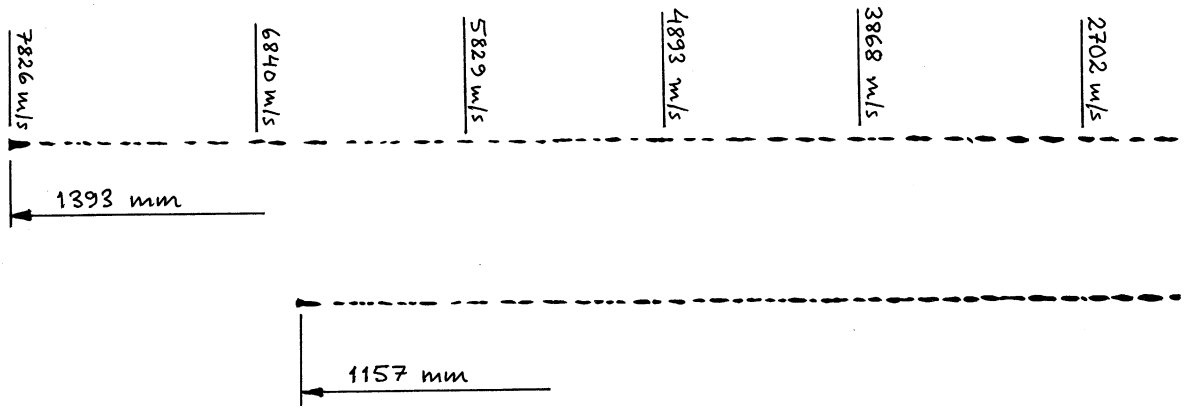

Figure 2: Two subsequent radiographs of a calibre *C*=80 mm SC jet without a metal liner around the explosive material. The thickness of the copper cone is *h*=1.9 mm and the apex angle is $2\theta=42^o$. The time delay between the first and the second radiograph is 30 μs. In the upper case the very first fragment is at the distance *S*≈17*C* or about three times the optimum stand-off from the SC.

Besides textbooks such as [1-3] there is a multitude of papers dealing with how projectiles and SC jets produce penetration. Nevertheless, two recent reports [4, 5] describe rigid projectile penetration and perforation, whereby the connection between these two cases appears to represent a new way of modelling. A following paper [6] suggests a quite new model for eroding projectile penetration. Furthermore this new model explains the transition between rigid and eroding projectile penetration in a natural way that agrees with experimental results.

Fragments in a SC jet are similar to small eroding projectiles. Accordingly, the present paper suggests how the model in [6] can be utilized to understand penetration reduction for PSC jets (and also for N-PSC jets) when $S>S_{opt}$.

Undeteriorated SC jet penetration

The suggested model for undeteriorated SC jet penetration is based on the model for eroding projectile penetration in [6]. Therefore, the relevant features of this model are first summarized below.

According to the model for eroding projectiles in [6] the penetration depth P depends on the yield strengths Y_P and Y_T and the corresponding densities ρ_P and ρ_T for the projectile and target materials, respectively. Deformation of the target material, so that a hole is produced with greater diameter D_T than the projectile diameter d_P, is assumed to correspond to a pressure $\beta_T Y_T$ over the hole bottom area $\pi D_T^2/4$, where the penetration coefficient is β_T=5. The hole depth P increases with the instantaneous velocity $u=dP/dt$. Consequently, the power required for hole production is given by $(\pi/4)D_T^2\,\beta_T\,Y_T\,u$. In the same manner, deformation of the projectile from the front end, so that it becomes a lining along the cylindrical hole wall, is assumed to correspond to the power $-(\pi/4)d_P^2\,\beta_P\,Y_P\,dL/dt$, where the projectile deformation coefficient β_P corresponds to melting of the projectile material and dL/dt is the rate at which projectile length is changed. The instantaneous projectile velocity is v. The relation between the velocities is $dL/dt=u-v$.

A basic assumption for the model in [6] is that the hole diameter is proportional to the (instantaneous) projectile velocity so that

$$D_T = d_P \frac{v}{v_T}, \tag{1}$$

where the characteristic velocity

$$v_T = \psi_T \sqrt{\frac{\beta_T\, Y_T}{\rho_T}}\,. \tag{2}$$

for the target material depends on the parameter ψ_T, which must be determined experimentally. For targets of aluminium, copper, steel and tungsten this parameter is found to be in the interval $1.1<\psi_T<1.5$ [6]. It should be emphasised that ψ_T may also depend on the projectile material, presumably so that it decreases in some manner with the ratio ρ_T/ρ_P, but for the time being such dependence is assumed to be negligible.

The model in [6] yields the instantaneous velocity

$$v_{\lim} = v_T \sqrt{\frac{1}{2}+\frac{\beta_T\, Y_T+(\beta_P-1)Y_P}{\rho_P\, v_T^2}+\sqrt{\left\{\frac{1}{2}+\frac{\beta_T\, Y_T+(\beta_P-1)Y_P}{\rho_P\, v_T^2}\right\}^2-\frac{2\,\beta_P\, Y_P}{\rho_P\, v_T^2}}} \tag{3}$$

above which the projectile produces a hole diameter that is large enough to make room for the eroded material. Thus, for $v>v_{\lim}$ the inequality

$$\left(D_T^2-d_P^2\right)u \geq -d_p^2\,\frac{dL}{dt} \tag{4}$$

is satisfied.

When $v>v_{\lim}$ the eroding projectile penetration is called *undisturbed*. When $v=v_{\lim}$ then $u=u_{\lim}=v_T^2/v_{\lim}$ and $D_T=D_{T,\lim}=d_P v_{\lim}/v_T$. For undisturbed eroding penetration the projectile length and velocity are both continuously reduced. When the impact velocity v_P is significantly higher than $v_{\lim}$, then the projectile length reduction effect dominates over the velocity reduction so that the velocity $v_{\lim}$ is reached when the projectile length is almost negligible (projectile erosion is almost complete). Accordingly subsequent penetration for $v<v_{\lim}$ is then quite negligible. It should be mentioned that the instantaneous relations

between the velocities u and v and the projectile length L are analytical, but that the penetration depth P, which is the time integral of u, must be determined via numerical integration.

When the impact velocity is only somewhat higher than $v_{\lim}$, then the instantaneous projectile velocity will be reduced to $v_{\lim}$ at some penetration depth $P_{\lim}$ for which the corresponding instantaneous projectile length $L_{\lim}$ is not negligible. This means that subsequent penetration must be governed by some modified model that accounts for the "squeezing" of eroded projectile material between the remaining projectile and the hole wall. The simple modification suggested in [6] is that $D_T=D_{T,\lim}$ as soon as $v<v_{\lim}$. When $v<v_{\lim}$ the eroding projectile penetration is called *disturbed*.

A fragmented SC jet may be assumed to consist of a stream of small packages of molten material from the SC insert. The pressure from an exploding SC on the insert is so high that the Hugoniot relations in combination with a realistic equation-of-state (EOS) for the insert material, and thermodynamics for the increase of temperature and entropy, should correspond to a final temperature above the melting point when the pressure has disappeared [1, 3]. Accordingly the projectile strength should be negligible so that $Y_P=0$. Then the model in [6] is considerably simplified. The projectile velocity v is constant and equal to the impact velocity v_P. The penetration velocity is also constant and given by

$$u=v_P\frac{\frac{\psi_T^2\,\rho_P}{2\,\rho_T}}{1+\frac{\psi_T^2\,\rho_P}{2\,\rho_T}}, \tag{5}$$

and the penetration depth becomes

$$P=\frac{1}{2}\psi_T^2\,\frac{\rho_P}{\rho_T}L_P\,. \tag{6}$$

The lengths of the fragments in a SC jet differ but they are all much smaller than the accumulated length L_P of the jet. The fragments are more like prolate ellipsoids than flat-ended cylinders, but here they will be assumed to have the latter shape. The shortest fragments have lengths of about a diameter, and the longest fragments have lengths of a few diameters. The real fragment diameters d_P are not constant but normally increase slightly towards the end of the jet [7], but here such increase will be neglected. It should also be emphasised that the diameter of the first fragment may be about twice as large as that of the second fragment, as in Figure 2, but this is also neglected here. Since the fragment velocities decrease along the jet so that the velocity of a fragment, behind which the remaining accumulated length is L, is given by $v\approx v_{front}L/L_P$, it follows that the hole should be approximately conical to the depth $P_{\lim}$ corresponding to the fragment velocity $v_{\lim}$ given by Eq. (3) with $Y_P=0$, namely

$$v_{\lim}=\sqrt{v_T^2+\frac{2\,\beta_T\,Y_T}{\rho_P}}=\sqrt{\beta_T\,Y_T\left(\frac{\psi_T^2}{\rho_T}+\frac{2}{\rho_P}\right)}\,. \tag{7}$$

For a SC jet of copper with $\rho_P=8.9\cdot10^3$ kg/m^3 and a target of hard steel with $\rho_T=7.8\cdot10^3$ kg/m^3, $Y_T=1.0$ GPa and parameter values $\psi_T=1.3$ and $\beta_T=5$ as in [4 - 6], Eq. (7) yields $v_{\lim}\approx1.5$ km/s. Since front velocities v_{front} of SC jets from conical inserts are in the range from 7 to 8 km/s it follows that most of the jet should produce a hole that is large enough to make room for the eroded jet material. After erosion by fragments with velocities that are only slightly higher than $v_{\lim}$, eroded projectile material, which in [6] is assumed to be deposited along the conical hole wall, will start to disturb the following fragments. However, for simplicity, it is assumed that penetration continues undisturbed as long as the fragment velocities are higher than $v_{\lim}$, and that subsequent penetration may be neglected.

As already mentioned above, the diameters of real SC jet fragments increase slightly towards the end of the jet. Furthermore, the jet is always terminated by a slug, which typically contains between 80 and 90% of the total mass of the insert in the SC. Thus the rear part of a SC jet and the slug will cause partial plugging of a hole in a target, unless the front part of the jet has been able to produce perforation with a sufficiently

large diameter to allow the slug to pass through. When a target has been penetrated but not perforated by a SC jet with a density that is close to the target density, then accurate determination of the maximum penetration depth P_{stop} requires that the target be cut (since radiographs yield little contrast when the density difference is small). According to the discussion and the assumptions above this depth should be given roughly by

$$P_{stop} \approx \frac{\psi_T^2 \, \rho_P \, L_P}{2 \, \rho_T} \left(1 - \frac{v_{\lim}}{v_{front}} \right). \qquad (8)$$

Deteriorated SC jet penetration

With the model suggested above for undisturbed SC jet penetration there is no mechanism that causes decreasing penetration depth P_{stop} with increasing stand-off $S>S_{opt}$. Accordingly, it is concluded that there must be a deterioration that becomes increasingly important with increasing distances between the fragments in a SC jet. Lateral dispersion and fragment rotation or deformation does not occur in free air. Hence hypothesis may be that a SC jet does not propagate as in free air inside the hole it makes in a target.

The model in [6] assumes that there is no detachment of target material during projectile penetration. The target material is deformed elastically-and-plastically to some diameter Λ_T that is typically at least $10D_T$. Outside this diameter the deformation is only elastic. If the elastic-plastic deformation is purely plastic, as it is commonly assumed to be, then the small elastic displacement immediately outside the elastic-plastic interface multiplied with $\pi\Lambda_T$ must be equal to the hole area $\pi D_T^2 / 4$, since plastic deformation occurs without significant change of volume. Since loose target material is not assumed to exist in the hole, such material cannot disturb a fragmented SC jet.

However, when a certain fragment enters the hole in the target, then the material of faster fragments, which previously created the hole by being eroded, is still present in the hole. These fragments-of-fragments should be moving in some highly stochastic manner but with velocities that are small compared to the initial velocities of the fragments from which they originate. It is quite unlikely that the eroded fragment material, which is certainly well molten, should be deposited along the hole wall so that it cannot interfere with subsequent fragments. This is contrary to eroded material from an eroding projectile, the temperature of which is initially close to the ambient temperature. When it is eroded against the bottom of the hole the temperature is assumed to instantaneously increase almost to the melting point. Thereby practically all strength is lost but the material may still not contain all the heat of fusion that is required to make it fully liquid. Eroded projectile material is normally found as a thin coating along the hole wall behind the residual projectile.

Before or just after SC jet fragmentation starts relatively slowly moving, already eroded, jet material may come in contact with the cylindrical surface of the (almost continuous) jet and should cause only negligible deterioration. But when the stand-off is significantly larger than optimal, then there is significant space between the fragments and some of the already eroded jet material may be struck by fragments that have not yet reached the bottom of the hole. Such impacts will cause much damage to the fragments, particularly since they can be expected to be in a molten state with negligible resistance against deformation. This effect will become more pronounced as the hole deepens. The reason is that the first fragments with high velocities create a large hole diameter, and consequently the density of eroded jet material is low close to the hole entrance, whereas this density increases along the hole in roughly inverse proportion to the decreasing hole cross section area. Thus, the deeper the hole, the higher is the density of disturbing material in the hole and the longer is the distance through the disturbing material before a fragment reaches the hole bottom and can contribute to the deepening of the hole. With this qualitative model for disturbance of fragmented SC jet penetration, the effect of the stand-off for $S>S_{opt}$ is understandable.

It seems difficult to design a quantitative physical model that describes this effect of stand-off for fragmented SC jets. However, such a model is hardly requested for practical applications, in particular in computer programs for assessment of effects and vulnerability of complex targets, such as tanks, fighters and naval ships that are subjected to SC jets. For such applications, a simple empirical model for the relation between penetration depth P and stand-off S that is similar to the one suggested in [7] should be quite sufficient, for instance

$$P(S)=\frac{5.6C}{1+\left(\frac{S-7C}{14C}\right)^2}. \qquad (9)$$

This relation yields a reasonably accurate description of the PSC graph in Figure 1. Thus $P(0)=P(14C)\approx 4.5C$, $P(21C)\approx 2.8C$ and $P(28C)\approx 1.7C$. The last value is slightly too high but at such large stand-off the relative experimental scatter in the penetration depth is almost ±50%. For modern PSCs with "trumpet-like" inserts, the maximum penetration is larger but the general behaviour as a function of stand-off is the same.

The N-PSC in Figure 1 is rather well described with a similar empirical relation, namely

$$P(S)=\frac{4.5C}{1+\left(\frac{S-C}{8C}\right)^2}. \qquad (10)$$

Eq. (10) yields $P(4C)\approx 3.9C$, $P(8C)\approx 2.5C$, $P(12C)\approx 1.6C$ and $P(24C)\approx 0.5C$.

Numerical simulation

Numerical simulation of the model suggested above is not straight-forward. An investigation with Autodyn and Lagrange mesh is reported in [8]. The jet consists of N=20 fragments of copper with the diameter d_P=2.0 mm and length l_P=2.5 mm, the first moving with the velocity v_{front}=8.0 km/s, the last with v_{end}=2.0 km/s and with linear velocity variation along the jet. The *(instantaneous) erosion strain* for both the jet and the target material is chosen to be 1.5. The target material is steel 4340 with the yield strength $Y_T\approx 0.8$ GPa. This and other material data, in particular the yield strength $Y_P\approx 0.09$ GPa for the jet material, are taken from the Autodyn catalogue.

When the effective strain in an element reaches the *erosion strain* the element is eroded, which means that the surface nodes of this element are detached from the rest of the mesh. The default setting in Autodyn is that the inertia (mass) of a detached node is removed, which in principle violates the fundamental requirement of continuity (or mass conservation). However, it is possible to keep the detached nodes (with mass) as free particles that fly around and interact, not with each other but with, e. g., hole walls and not yet completely eroded SC jet fragments. When eroded nodes are removed, then all fragments are intact when they reach the bottom of the hole and always produce a significantly deeper hole than when the detached nodes remain in the hole. Below all results are calculated without removal of eroded nodes, except in one case where the eroded nodes are either kept or removed in order to demonstrate the difference. It should be emphasised that the mass of an eroded node is directly determined by the numerical mesh, whereas real eroded material can be produced in smaller as well as greater pieces.

If the jet is continuous (accumulated length equal to real length Nl_P=50 mm) when the first fragment impacts the target, then the calculated penetration depth is P=70.9 mm. In this case jet stretching continues and fragmentation of the residual jet during penetration may occur due to the combined effect of the initial velocity gradient and the chosen value for the *erosion strain*.

If the initial separation between fragments is zero when the first fragment impacts the target, then the calculated penetration depth is P=60.6 mm. Thus, continued stretching of the continuous jet yields a larger effective projectile length L_P, so that the penetration depth P=70.9 mm is reached, whereby the jet is thinner and the hole diameter is smaller than for the initially fragmented jet.

If the initial separation between fragments is s=1.0 mm when the first fragment impacts the target, then the calculated penetration depth is P=54.8 mm. If the eroded nodes are removed, so that the fragments are not partly destroyed on their way to the hole bottom, then the penetration depth is P=63.7 mm or about 16% greater. For larger initial separation (larger stand-off) and a higher number of fragments the difference must be larger. The latter statement is validated by Figure 3. The 18th fragment has just entered the hole, where the density of eroded material is negligible so that this fragment is still intact. The fragment separation has grown from the initial value to about $(v_{front}-v_{end})(s+l_P)/v_{end}-l_P\approx 8$ mm. Erosion of the 17th fragment is only just visible, whereas the 16th fragment already is almost completely destroyed by previously eroded

material. Accordingly, additional fragments will not contribute to the penetration depth. Thus, the difference to a not fragmented jet increases rapidly with the number of fragments.

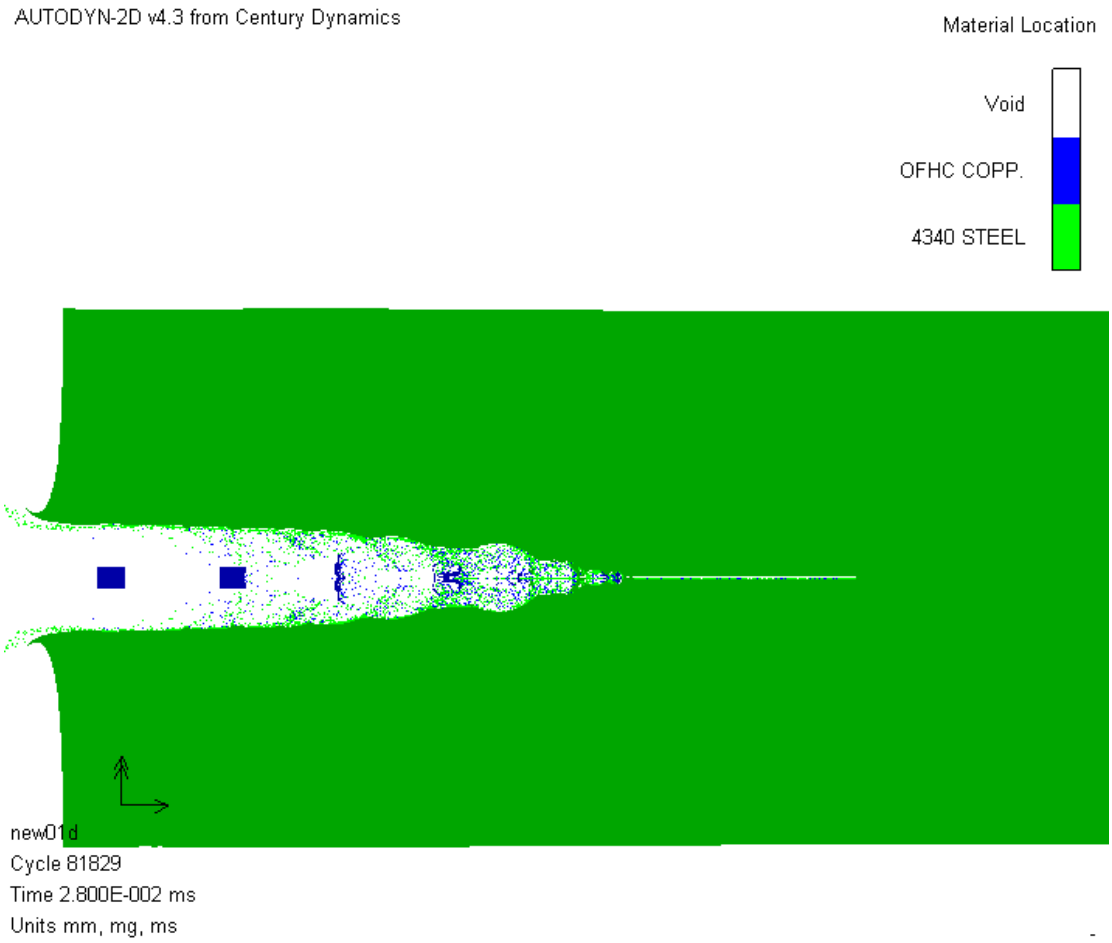

Figure 3. The 18th of 20 fragments, with diameter 2.0 mm and length 2.5 mm, and with initial separation s=1.0 mm has just entered the hole produced by the previous fragments.

The initial separations 2.0 and 5.0 mm yield P=50.3 and 48.3 mm, respectively. The number of eroded target nodes seems to be about equal to the number of eroded jet nodes. In this respect the calculations differ from the suggested model, in which there is no erosion but only elastic-plastic deformation of the target. The later fragments in the jet are severely eroded from their front ends by the eroded nodes that they encounter. Consequently the anticipated disturbance is obvious and should explain at least most of the decrease of $P(S)$ for $S>S_{opt}$ in Figure 1.

With the calculated penetration depth P=63.7 mm for a SC jet of undeteriorated and non-stretching fragments with the accumulated length $L_P=20l_P=50$ mm, Eq. (6) yields $\psi_T\approx1.50$. This is practically equal to the experimental result $\psi_T\approx1.46$ in [6] for copper projectiles eroding targets of the same copper material. However, it was also shown in [6] that the target size in the lateral directions was far too small to simulate a semi-infinite target. When the target is too small, then probably both the penetration coefficient β_T and the hole size parameter ψ_T are smaller than for a semi-infinite target. As a matter of fact the target is actually too small in the numerical calculations in [8], at least according to [6] where the outer diameter Ω of the target is required to be at least somewhat larger than the radius Λ_T for plastic deformation of the target material. This requirement typically corresponds to $\Omega_{min}>15D_T$. In [8] the diameter ratio is chosen to be rather small, namely Ω=50 mm so that $\Omega/D_T\approx5$, in order to reduce the calculation time. The lateral expansion of the target is small but visible in Figure 3, where the maximum expansion does not occur at the corners to the left but for larger depth. The reason is that for smaller depth upheaval of the impacted surface requires less energy than radial expansion.

The spurious, very narrow hole ahead of the "real" hole to the right in Figure 3 is a numerical defect caused by eroded projectile (and target) nodes that reach the axis and accumulate there. When eroded nodes are removed the spurious hole disappears.

Other experimental results for ψ_T in [6] are $\psi_T \approx 1.1$ for tungsten projectile erosion of steel, $\psi_T \approx 1.3$ for steel projectile erosion of aluminium, $\psi_T \approx 1.3$ for steel projectile erosion of steel and $\psi_T \approx 1.5$ for tungsten projectile erosion of tungsten. It is suspected that the model for the hole diameter in Eqs. (1) and (2), where ψ_T depends only on the target material, is too simple. From the results for steel and tungsten projectiles eroding steel targets it seems that ψ_T should decrease with the ratio ρ_T/ρ_P. This would be logical since an outwards flow of higher density material should result in a larger hole diameter, which corresponds to a smaller ψ_T. However, for the time being there is not sufficient experimental information for quantitative evaluation of this proposal.

Experimental results

For one of the SC:s in [7, Figure 2] the calibre is C=92 mm, the insert diameter is D=77 mm, the apex angle of the conical insert is 2θ=42° and the thickness of the insert is h=2.3 mm. Thus the volume of the insert is $V \approx \pi h D^2/\{4\sin(\theta)\} \approx 30$ cm^3. The half-hole profiles produced with this SC in steel 1311 at stand-off S=15, 60 and 160 cm are shown in Figure 4.

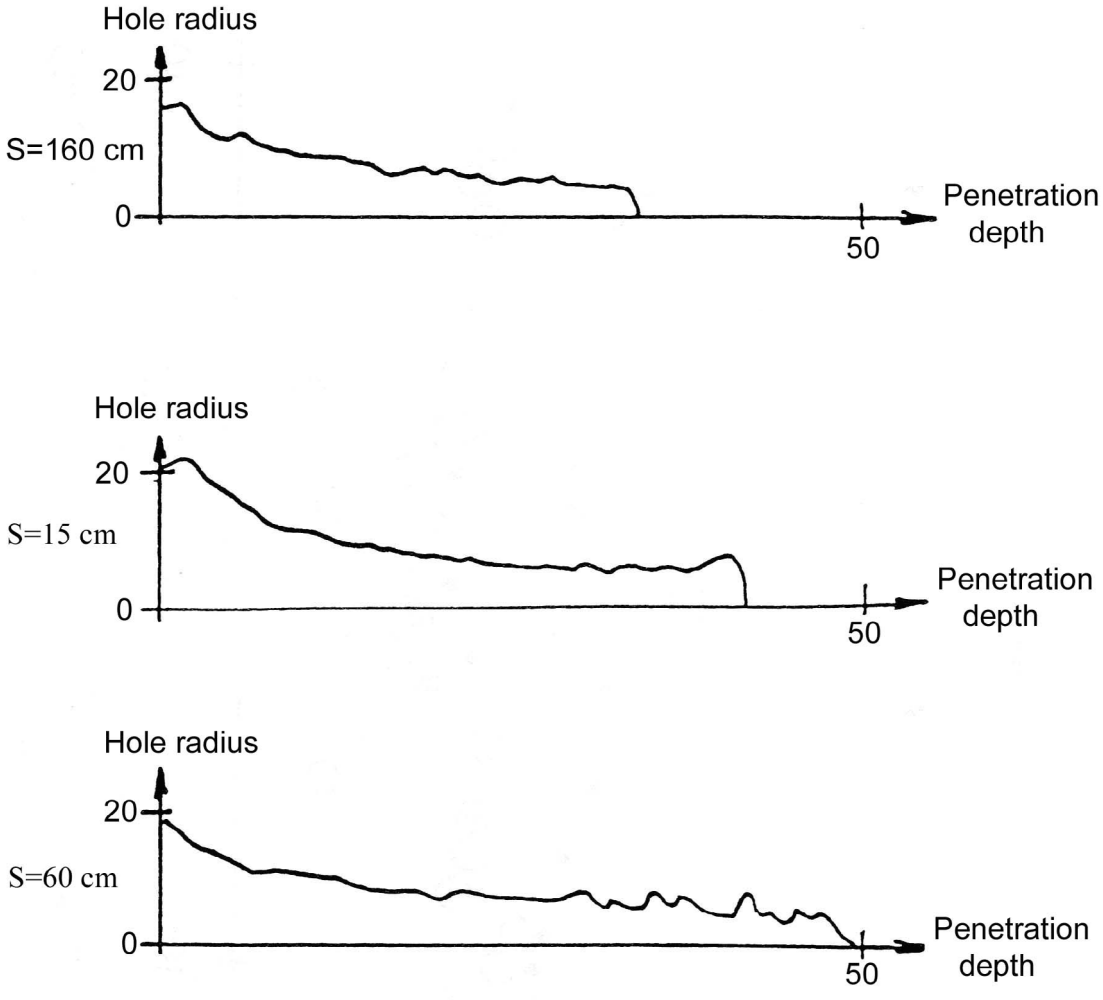

Figure 4. Half-hole profiles in steel SIS 1311 produced by SC jets with calibre *C*=92 mm at three stand-off distances *S*. The base diameter of the conical insert is *D*=77 mm, the half apex angle is θ=21° and the insert thickness is *h*=2.3 mm. Hole radius and penetration depth are in mm.

For the somewhat different SC in [7, Figure 3], which is copied in Figure 5, the design data are D=72 mm, 2θ=50° and h=1.9 mm. Thus the volume of the insert is $V \approx \pi h D^2/\{4\sin(\theta)\} \approx 18$ cm^3. The velocity of the first fragment is $v_{front} \approx 6.9$ km/s. A representative value for the diameter of the first 30 fragments is

$d_P \approx 1.5h \approx 2.8$ mm. From the next fragment, for which the velocity is $v \approx 3.9$ km/s, the diameter increases to $d_P \approx 2.0h \approx 3.8$ mm for fragment number 40, for which the velocity is $v \approx 2.8$ km/s. The diameter and velocity of the 47th and last measured fragment are $d_P \approx 3.0h \approx 5.7$ mm and $v \approx 2.0$ km/s. The estimated total mass of these fragments in [7, Figure 4] is 30 g. Thus the volume $30/7.8 \approx 3.8$ cm^3 of these fragments corresponds the fraction α=21% of the insert volume.

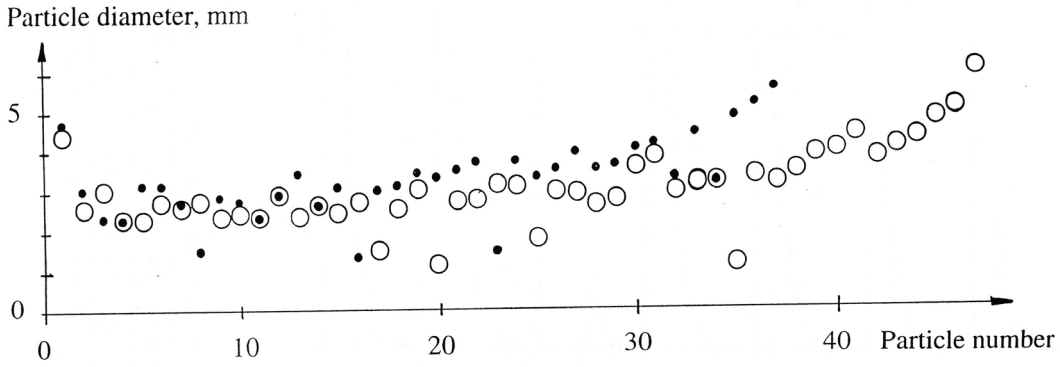

Figure 5. Average SC jet fragment diameter produced by two different explosives and identical conical inserts of copper. The insert base diameter of the insert is D=77 mm, the half apex angle is θ=21^o and the thickness is h=2.3 mm. For the circles and points the first fragment velocity is $v_{front} \approx$6.9 km/s and 5.7 km/s, respectively.

When the stand-off is S=60 cm or $S \approx 6.5C$ for the C=92 mm SC in Figure 4, then the initial diameter of the hole is $D_T \approx 38$ mm and the penetration depth is $P \approx 5.2C \approx 48$ cm. When the stand-off is S=160 cm or $S \approx 17C$, then the initial diameter of the hole is still $D_T \approx 38$ mm, as it should be since it is produced by the first fragments in the jet, and the penetration depth is $P \approx 3.7C \approx 34$ cm. Thus, according to Figure 1 and Eq. (8) the SC considered in Figure 4 is (quite close to) a PSC.

In Figures 2 and 5 the diameter of the very first fragment is about twice that of the following fragments. This is neglected when Eq. (1) is used to calculate the initial diameter of the hole in the target.

The target material in Figure 4 is a soft steel SIS 1311 for which $Y_T \approx 0.3$ GPa. With β_T=5 and ψ_T=1.3 from [6] Eqs. (2) and (7) yield $v_T \approx 0.6$ km/s and $v_{\lim} \approx 0.8$ km/s. It is reasonable to assume that the ratio d_P/h for the SC in Figure 4 should be quite close to that of the SC in Figure 5. Furthermore, since the insert apex angles are equal for the SC:s in Figures 2 and 4 it is reasonable to assume that the first fragment velocity should be equal, at least with the same explosives. With d_P/h=1.5 and $v_{\text{front}} \approx 7.8$ km/s Eq. (1) yields $D_T \approx 45$ mm for the SC in Figure 4. With a somewhat smaller ratio or a somewhat smaller first fragment velocity, which perhaps is more likely with regard to the effect of different explosives in Figure 5, the calculated diameter is equal to the experimental result.

A rough average fragment cross sectional area for the fragmented jet in Figure 5 is $\pi\{30 \cdot 1.5^2 + 10(1.5^2+2.0^2)/2 + 7(2.0^2+3.0^2)/2\}h^2/188 \approx 8.7$ mm^2. With the same relation between fragment area and insert thickness and same fraction α=21% for the SC in Figure 4 the estimated length of the jet is $L_P \approx 49$ cm. Since $v_{\lim} \approx 0.8$ km/s is smaller than the velocity of the last (47th) fragment the parenthesis in Eq. (8) should be unity. With ψ_T=1.3 for steel from [6] Eq. (7) then yields $P_{stop} \approx 47$ cm, which is close to the corresponding experimental value $P \approx 48$ cm for the stand-off S=60 cm in Figure 4. This stand-off is quite close to the optimum stand-off in Eq. (9), namely $S_{opt} \approx 7C \approx 64$ cm, from which the maximum penetration $P(7C) \approx 52$ cm is expected. Accordingly both results from Eqs. (8) and (9) are in reasonable agreement with the experiment. However, it is possible that the non-measured fragments with velocities in the interval from $v_{\lim}$ to 2.0 km/s also contribute to the final penetration depth. On the other hand, it is also likely that the fraction α=21% for the SC in Figure 5 is larger than for the SC in Figure 4.

Experimental results for C=45 mm SC copper jets in targets of steel SIS 1311 and aluminium are reported in [9]. Results with the same SC in targets of steel KATF 415-8 are reported in [10]. The insert diameter is D=40 mm, the half apex angle of the conical insert is θ=25^o and the thickness of the insert is h=1.06 mm. Thus the volume and mass of the insert are $V \approx \pi h D^2/\{4\sin(\theta)\} \approx 3.1$ cm^3 and 28 g, respectively. The velocity of the first fragment is $v_{front} \approx 7.6$ km/s and the velocity decreases linearly with the accumulated fragment length to $v \approx 3.0$ km/s for $L_P \approx 32$ cm, which corresponds to the accumulated fragment mass 2.5 g [11]. Accordingly the calculated fragment diameter $d_P \approx 1.1$ mm is practically equal to the insert thickness h for this SC. For targets of steel SIS 1311 with $v_T \approx 0.6$ km/s Eq. (1) yields the initial hole diameter $D_T \approx 14$ mm.

In [9] the three experimental results at stand-off S=80 mm are D_T≈15, 18 and 18 mm. Since the SC jet stretching continues until optimum stand-off S_{opt}≈30 cm Eq. (1) should underestimate the initial hole diameter.

Two aluminium target qualities with yield strength Y_T≈0.25 and 0.37 GPa were investigated in [9]. Three or four holes were produced in each material at each stand-off S=80, 400 and 800 mm. The average of the initial hole diameter differs negligibly from D_T≈17 mm for all cases. Penetration depth at optimum stand-off S_{opt}≈7C≈30 cm is estimated to be $P(S_{opt})$≈35 and 31 cm, respectively. For simplicity it is assumed that the two aluminium qualities can be regarded as one with the yield strength Y_T≈0.3 GPa, that $P(S_{opt})$≈(35+31)/2=33 cm and that the latter corresponds to P_{stop} in Eq. (7) with the parenthesis equal to unity. Accordingly Eq. (7), L_P=32 cm and P_{stop}=33 cm yield ψ_T≈0.77, whereupon Eqs. (1) and (2) and D_T=17 mm yield β_T≈3.7. Both are significantly smaller than the corresponding values for eroding penetration with steel projectiles in targets of similar aluminium in [6], namely ψ_T≈1.15 and β_T≈6.0.

The results in [10, Diagram 1], which is copied in Figure 6, show large difference between soft steel SIS 1311 and hard steel KATF 415-8, for which Y_T≈0.8 GPa. For stand-off distances S≤4C penetration is about equal to PSC in Figure 1. For larger stand-off penetration in SIS 1311 first exceeds PSC in Figure 1 to become about equal for S=20C, whereas penetration in KATF 415-8 drops rather abruptly to be only somewhat larger than for N-PSC for S≥10C in Figure 1.

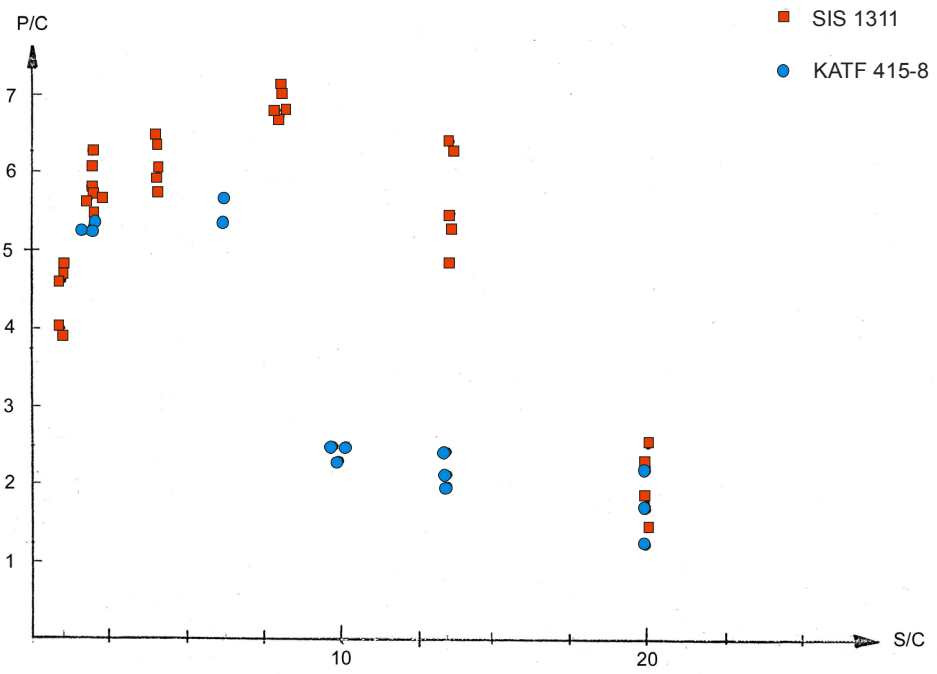

Figure 6. Penetration depth *P* as function of stand-off *S* for *C*=45 mm SC jets in soft steel SIS 1311 and hard steel KATF 415-8 from [10, Diagram 1].

The average initial hole diameter in KAFT 415-8 is D_T≈15, 14 and 15 mm for S/C=2, 6 and 8 [10, Table 9 - 11]. Accordingly d_P≈1.1 mm, v_{front}≈7.6 km/s [11], β=5 and Eqs. (1) and (2) yield ψ_T≈0.8.

Two conclusions in [10] are that *for small stand-off the hole diameter in KATF 415-8 is 2 - 3 mm smaller than in SIS 1311* and that *for large stand-off there is large variation in the hole diameter*.

Discussion

It should be emphasised that fragment velocities in the first part of a SC jet are always are higher than the fundamental elastic wave velocities in target material. In steel as well as in aluminium the elastic dilatation and distorsion wave velocities are about 6 and 3 km/s, respectively. This is a reason to expect that the model in [6], for ordinary eroding projectiles with velocities that are at most about 1.8 km/s, may have to be modified before it can be used to describe SC jet penetration. Nevertheless this model appears to yield both

penetration depth and hole diameter in targets of steel with acceptable accuracy for SC:s with copper inserts at suboptimal stand-off.

The corresponding results for aluminium targets are less satisfactory. The smaller value of ψ_T with SC jets corresponds to larger hole diameters. Here it should be mentioned that projectiles of tungsten produce larger holes in steel targets, corresponding to $\psi_T \approx 1.1$, than projectiles of steel for which $\psi_T \approx 1.3$ [6]. Therefore it is suggested in [6] that ψ_T should decrease with the ratio ρ_T/ρ_P since the outwards flow of heavier eroded projectile material at the hole bottom can be imagined to produce larger hole diameter, but this cannot explain the difference above between the ψ_T-values for aluminium with either eroding projectiles of steel or SC jet fragments of copper.

The relatively small value $\beta_T \approx 3.7$ of the penetration coefficient for SC jets is even more disturbing. However, there is a significant difference between the aluminium targets considered in [6] and in [9], namely that the latter are solid whereas the former consist of stacks of 10 mm thick plates. It should be easier produce a hole in stacked targets, which means that either β_T or ψ_T or both should be smaller than for a solid target, but it is indeed questionable if the differences should be as large as above.

In Autodyn calculations already eroded nodes erode the jet fragments that have not yet reached the hole bottom, and this is (assumed to be) the primary reason why the penetration depth $P(S)$ decreases with increasing stand-off S for $S>S_{opt}$. In reality it is likely that there is not only elastic-plastic deformation of the target but that a minor part of the material that initially occupied the hole space (presumably close to the axis), is eroded and mixed with the eroded jet material, as pictured in the numerical calculations without removal of eroded nodes in Figure 3. The density of eroded material in the hole increases with the hole depth since the hole diameter decreases with the velocities of the eroding fragments. Consequently the contribution P_n from the fragment with number n to the accumulated penetration depth decreases with increasing n since the length reduction of a fragment before it reaches the hole bottom increases with n.

Furthermore, since the hole depth decreases but the diameter does not increase with increasing stand-off, as seen in Figure 4, the density of already eroded SC jet material increases progressively with increasing n. For some number n all following fragments will be completely pre-eroded before they reach the hole bottom. This explains why the penetration depth almost vanishes when the stand-off is several times larger than optimum.

In the numerical calculations the SC jet fragments have the non-vanishing strength Y_P=0.09 GPa, whereas it is assumed in the model that the material is molten. It is likely that fragment erosion by collisions with detached nodes is more destructive if Y_P=0. On the other hand, when Y_P=0 more energy is available for penetration when a fragment reaches the hole bottom. To investigate this question the case with 1.0 mm initial separation was recalculated with Y_P=0 and resulted in a marginal penetration reduction from P=54.8 to 52.2 mm.

A principal problem with the numerical calculations is that they are carried out for an axially symmetric situation. Thus a detached node is a material ring, which only keeps its shape if it moves along the axis (the upper and lower halves of Figure 3 are mirror images). If a ring has an outwards radial velocity component, then it becomes stretched and if it reaches the hole wall it (seems as if it) bounces against the wall. If it has an inwards radial velocity component, then it is compressed and compression becomes infinite if it reaches the axis instead of colliding with a fragment. Furthermore, it does not bounce against the axis but appears to become stuck there. This seems to be the reason for a spurious effect, namely a “hole” along the axis that is only one mesh element wide and extends far beyond the bottom of the hole. This hole is absent when the calculations are carried out for a two-dimensional, plane strain situation. It would also be absent in a three-dimensional calculation.

Conclusions

The decrease of the penetration depth for Shaped Charges with increasing stand-off beyond optimum is a well known effect. To the authors’ knowledge, primarily based on text-books, the common explanation is lateral dispersion and rotation of the jet fragments, despite the experimental fact that such effects are not observed for jets in free air at relevant distances. The explanation suggested in the present paper, namely that later parts of the jet become increasingly eroded by previously eroded parts before these later part can contribute to the penetration, appears to be new and is easily understandable and physically realistic.

The model for Shaped Charge jet penetration is a natural extension of a previously suggested model for eroding projectiles with much smaller velocities than those of most of the fragments in a Shaped Charge jet. It seems as if both the penetration depth and the hole diameter from a Shaped Charge, at or close to

optimum stand-off where there is negligible deterioration of the residual jet by previously eroded jet material, can be reasonably well predicted with the target parameter values obtained from projectile experiments. However, choosing values for the most critical parameters, namely the target yield strength Y_P and the non-dimensional hole size parameter ψ_T, is far from trivial.

References

1. W: P. Walters & J. A. Zukas, *Fundamentals of shaped charges*, John Wiley & Sons, New York 1989.
2. J. Carleone, *Tactical Missile Warheads*. American Institute of Aeronautics and Astronautics, IAAA Vol. 155, 1993.
3. M. A. Meyers, *Dynamic Behaviour of Materials*. John Wiley & Sons, New York (1994).
4. G. Wijk, M. Gustafsson & A. Tyrberg, A model for rigid projectile penetration and perforation of hard steel and metallic targets, Swedish Defence Research Agency, FOI-R--1617--SE, April 2005.
5. G. Wijk, Initially increasing penetration resistance, friction and target size effects in connection with rigid projectile penetration and perforation of hard steel and metallic targets, Swedish Defence Research Agency, FOI-R--1631--SE, April 2005.
6. G. Wijk, A model for eroding projectile penetration of metallic targets, submitted to *International Journal of Impact Engineering,* June 2005.
7. G. Wijk, A new mathematical model for the relation between stand-off and penetration of shaped charge jets. Swedish Defence Research Agency, F0I-R--0361--SE, January 2002.
8. A. Tjernberg, Simulering av fragmenterade rsv-strålars penetrationsförmåga, F0I-R--1313--SE, September 2004.
9. J. Ekberg, RSV mot aluminium. Swedish Defence Research Agency, FOA rapport C 20348-D4, Mars 1980.
10. J. Ekberg, RSV mot stålpansar. Swedish Defence Research Agency, FOA rapport C 20406-D4, April 1981.
11. Å. Collin, Swedish Defence Research Agency FOI (private communication).